PHYSICAL REVIEW A VOLUME 46, NUMBER 5 1 SEPTEMBER 1992

Electron-positron pair creation with capture and ionization in relativistic heavy-ion collisions by the finite-difference method

Joachim Thiel, Alex Bunker, Klaus Momberger, Norbert Grün, and Werner Scheid
Institut für Theoretische Physik der Justus-Liebig-Universität, Giessen, Germany
(Received 23 December 1991)

The probabilities of electron-positron pair creation with K-shell capture, of ionization, and of excitation are nonperturbatively calculated with a finite-difference method. Calculations for a collision of U^{92+} on U^{91+} at $E_{\rm lab}$= 10 GeV/nucleon at small impact parameters are presented. The results show an enhancement of the probability for pair creation with capture of about two orders of magnitude in comparison to the outcome of a calculation in first-order perturbation theory. This proves the expected strong nonperturbative character of such relativistic collisions for very heavy ions.

PACS number(s): 34.50.Fa, 14.60.Cd, 02.70.+d

I. INTRODUCTION

Lepton pair production in relativistic heavy-ion collisions has been studied in the past years with increasing interest. The electron-positron pair creation with capture of the electron into a bound state leads to a change of the charge of the beam ions and is therefore of particular interest for the design of superrelativistic heavy-ion colliders, because the recharged ions get lost from the beam [1].

In the high-energy limit the electron-positron pair creation can be calculated by the equivalent-photon method [2, 3], which assumes the Lorentz-contracted electromagnetic fields of the heavy ions as pulses of photons. The cross section for the production of pairs is then given by the elementary two-photon cross section for this process multiplied by the number of photons in these pulses. In the case of relativistic collisions of projectiles with lower charge numbers ($Z_P \approx 1$) and larger impact parameters, perturbation theory is applicable to the calculation of pair creation [4–7]. The various perturbative calculations are different with respect to the wave functions of the initial and final states. Also nonperturbative calculations were made with the help of B-spline methods [8] and in the framework of coupled-channel calculations which were applied to ionization, excitation, and charge transfer [9–14]. The coupled-channel calculations showed an enhancement of about two orders of magnitude in the pair creation probability compared with the results of the perturbation theory for relativistic collisions of very heavy ions (Au+Au, U+U) at small impact parameters. A reason for this enhancement is the large value of $Z_P\alpha$ which for a uranium projectile amounts to 0.67. Since this coupling is large for very heavy systems like U+U and small impact parameters, perturbative treatments might fail and higher-order effects and multiple pair creation could become important [4, 15–20].

The aim of this paper is the calculation of pair production with capture by solving the time-dependent Dirac equation with the finite-difference method. This method was first applied by Becker *et al.* [21] to the process of excitation and ionization in relativistic heavy-ion collisions. To simplify the numerical procedure the method is presently restricted to problems with rotational symmetry with respect to the internuclear axis, which can be regarded as a very good approximation to nearly central collisions. We compare our results with those of the coupled-channel method which in turn has the deficiency to be restricted in the number of channels taken into account.

In Sec. II we discuss the semiclassical treatment and the numerical procedure for the calculation of the probabilities of pair production with capture into the K shell. Section III gives the results for ionization and pair production with capture for collisions of U^{92+} on U^{91+} and U^{92+}, respectively, at $E_{\rm lab} = 10$ GeV/nucleon.

II. SEMICLASSICAL APPROACH AND NUMERICAL METHOD

We make use of the semiclassical approximation, which treats the motion of the nuclei classically and the electron motion by quantum mechanics with the time-dependent Dirac equation

$$i\hbar \frac{\partial}{\partial t} \Psi(\mathbf{r},t) = \{ c\boldsymbol{\alpha} \cdot [\mathbf{p} + (e/c)\mathbf{A}(\mathbf{r},t)] + \beta mc^2 - eV(\mathbf{r},t)\}\Psi(\mathbf{r},t), \qquad (1)$$

where $\Psi(\mathbf{r},t)$ denotes the four-component Dirac spinor and $\boldsymbol{\alpha}$ and β the Dirac matrices; $\Psi(\mathbf{r},t)$ can be interpreted as the electron-positron field. The classical fields $\mathbf{A}(\mathbf{r},t)$ and $V(\mathbf{r},t)$ contain the electromagnetic potentials of the target and projectile nucleus. We assume that the projectile nucleus moves with constant velocity v along the z axis and the target nucleus is fixed at $z = 0$. Then in the case of extended spherical target and projectile charges with homogeneous charge densities, charge numbers Z_T and Z_P, and radii R_T and R_P, respectively, the potentials are given by

$$V(\mathbf{r},t)=eZ_T f_T(r)+eZ_P\gamma f_P(r'), \tag{2}$$

$$\mathbf{A}(\mathbf{r},t)=eZ_P(v/c)\gamma f_P(r')\mathbf{e}_z, \tag{3}$$

where $\gamma = 1/(1-v^2/c^2)^{1/2}$ is the Lorentz factor, $r' = [x^2+y^2+\gamma^2(z-vt)^2]^{1/2}$, and f_n is given by $(n=T,P)$

$$f_n = \begin{cases} 1/r, & r \geq R_n \\ (3-r^2/R_n^2)/2R_n, & r \leq R_n. \end{cases} \tag{4}$$

The impact parameter b is set equal to zero. Thus, we have to solve a rotationally symmetric problem with the finite-difference method. The rotational symmetry allows the reduction of the numerical solution of Eq. (1) to a two-dimensional grid. The numerical method and tests of the accuracy are published by Becker *et al.* [21] and will not be repeated here.

We start the numerical calculation with the analytically given exact $1s_{1/2}$ bound-state solution of the target Hamiltonian for a point charge $Z_T e$ located at $z = 0$. After the time evolution of this wave function with Eq. (1) we project the result on the analytically given eigenstates of the target Hamiltonian with the target point charge. By projecting on excited bound states we get the probability for excitation and by projecting on the positive and negative continuum states the probability for ionization and pair production with capture in the $1s_{1/2}$ bound state, respectively. In the latter case we apply time-reversal symmetry.

The use of eigenfunctions of a Hamiltonian for a point charge for the initial and final states on the one hand and potentials of extended charges for the time evolution on the other hand is somewhat inconsistent, but the latter extension of the charges can be understood as a regularization of the potentials at $r = 0$ and $r' = 0$, respectively. As test calculations for the time evolution of the $1s_{1/2}$ bound-state wave function without distortion by a projectile potential have shown, this regularization helps to hold the solution stable on the grid.

In order to obtain the probabilities for excitation P_e, ionization P_i, and pair production with capture in the $1s_{1/2}$ bound state P_p, we have to project the time developed wave function after the collision on the final states. In the case of excitation we use exact analytic solutions $|n,\kappa\rangle$ of the target Hamiltonian for a point charge [22], which are classified by the quantum numbers n and κ. Because of the assumed cylindrical symmetry of the problem the j_z value remains constant in time and all functions (initial and final) are taken for $j_z = \frac{1}{2}$. The excitation probability is calculated as

$$P_e = \sum_{\kappa=\pm 1}^{\pm\infty} \sum_{n=n_{\min}}^{\infty} |\langle n\kappa \mid f\rangle|^2 - |\langle 1s_{1/2} \mid f\rangle|^2, \tag{5}$$

with $n_{\min}(\kappa) = |\kappa| + (\kappa+|\kappa|)/2\kappa$ and $\mid f\rangle = \mid \Psi(t\to\infty)\rangle$. The ionization and pair-production probability can be obtained by projecting with exact continuum eigenfunctions $|E,\kappa\rangle$ of the Coulomb problem for the charge $Z_T e$ ("ex" means exact target eigenfunctions):

$$\begin{aligned} \frac{dP_i^{\text{ex}}}{dE} &= \sum_{\kappa=\pm 1}^{\pm\infty} |\langle E,\kappa \mid f\rangle|^2 \quad \text{for} \quad E \geq m_0c^2, \\ \frac{dP_p^{\text{ex}}}{dE} &= \sum_{\kappa=\pm 1}^{\pm\infty} |\langle E,\kappa \mid f\rangle|^2 \quad \text{for} \quad E \leq -m_0c^2, \end{aligned} \tag{6}$$

$$\begin{aligned} P_i^{\text{ex}} &= \int_{m_0c^2}^{\infty} \frac{dP_i^{\text{ex}}}{dE} dE, \\ P_p^{\text{ex}} &= \int_{-\infty}^{-m_0c^2} \frac{dP_p^{\text{ex}}}{dE} dE. \end{aligned} \tag{7}$$

In the following we restrict the representation of the formulas to the ionization probability. Similar formulas hold for the pair-production probability. As we will show later on, the exact target eigenfunctions with the quantum numbers κ are not the optimum basis states to describe ionization with a high linear momentum of the ionized electron in the forward direction. In this case projection probabilities of many high κ values ($|\kappa| > 10$) have to be summed up. These projection probabilities are calculated with continuum functions of high energy, which are difficult to compute with sufficient accuracy. Therefore, we decided to project with Sommerfeld-Maue functions (SMF's) [22–24]. These functions are approximate solutions of the target Hamiltonian, which in the form used here contain an incoming spherical wave and a plane wave with linear momentum $\mathbf{p}$ and helicity μ. As shown by Bethe and Maximon [25], the shortcoming of the Sommerfeld-Maue functions compared with the exact solutions is of the order $O((Z\alpha)^2/l)$. Therefore, these functions can be used to describe ionization and pair production at high linear momentum values of the ionized electron or created positron, respectively. However these wave functions are not orthogonal, since two functions $|\mathbf{p}_1,\mu_1\rangle, |\mathbf{p}_2,\mu_2\rangle, \mathbf{p}_1 \neq \mathbf{p}_2, \mu_1 \neq \mu_2$ fulfil the relation $\langle \mathbf{p}_1,\mu_1| \; E_1 + E_2 + 2Ze^2/r \; |\mathbf{p}_2,\mu_2\rangle = 0$, with $E_i = [\mathbf{p}_i{}^2c^2 + (m_0c^2)^2]^{1/2}, i = 1,2$. Nevertheless we assume that these functions form an orthonormal set normalized as

$$\langle \mathbf{p}_1,\mu_1|\mathbf{p}_2,\mu_2\rangle = \delta(\mathbf{p}_1-\mathbf{p}_2)(\mathbf{p}_1-\mathbf{p}_2)\delta_{\mu_1\mu_2}. \tag{8}$$

We obtain in the case of Sommerfeld-Maue functions

$$\frac{d^3P_i^{\text{SMF}}}{d^3p} = \sum_{\mu=-1/2}^{1/2} |\langle \mathbf{p},\mu \mid f\rangle|^2. \tag{9}$$

Because of the cylindrical symmetry of the problem we can write

$$\frac{d^2P_i^{\text{SMF}}}{dp_l dp_t} = 2\pi\, p_t \sum_{\mu=-1/2}^{1/2} |\langle p_l,p_t,\mu \mid f\rangle|^2, \tag{10}$$

where p_l and p_t are the longitudinal and transversal momenta, respectively. This can be rewritten in the form

$$\frac{dP_i^{\mathrm{SMF}}(E)}{dE} = E\,2\pi \int_0^{p=\{E^2-(m_0c^2)^2\}^{1/2}} \frac{p_t}{\sqrt{p^2-p_t^2}}\,\frac{d^3P_i^{\mathrm{SMF}}(+\sqrt{p^2-p_t^2},p_t)}{d^3p}\,dp_t + E\,2\pi \int_0^{p=\{E^2-(m_0c^2)^2\}^{1/2}} \frac{p_t}{\sqrt{p^2-p_t^2}}\,\frac{d^3P_i^{\mathrm{SMF}}(-\sqrt{p^2-p_t^2},p_t)}{d^3p}\,dp_t. \tag{11}$$

A further assumption is the completeness of the set $\{|E,\kappa\rangle, |E|<E_0\}\cup\{|\mathbf{p},\mu\rangle, |E(\mathbf{p})|\geq E_0\}\cup\{|n,\kappa\rangle\}$, where E_0 is the energy up to which exact solutions give us a good description of the ionization and pair production. Above this energy the Sommerfeld-Maue functions are a good approximation to the exact solutions. The value of this energy E_0 will be fixed later. Under this assumption the ionization probability is finally given by

$$P_i = \int_{m_0c^2}^{E_0} \frac{dP_i^{\mathrm{ex}}}{dE}dE + \int_{E_0}^{\infty} \frac{dP_i^{\mathrm{SMF}}}{dE}dE\,. \tag{12}$$

Similary the pair production probability is given by

$$P_p = \int_{-E_0}^{-m_0c^2} \frac{dP_p^{\mathrm{ex}}}{dE}dE + \int_{-\infty}^{-E_0} \frac{dP_p^{\mathrm{SMF}}}{dE}dE\,, \tag{13}$$

where the differential probabilities are defined in analogy to the differential ionization probabilities. In the following we also use the quantities $P_e(t)$, $P_x^{\mathrm{ex}}(t)$, and $P_x^{\mathrm{SMF}}(t)$, with $x\in\{i,p\}$ and their differentials. These quantities are defined by Eqs. (5), (12), and (13) if we replace the final state $\mid f\rangle$ by the state $\mid \Psi(t)\rangle$. They give us information about the behavior of the wave function during the time evolution and allow comparisons with other procedures, i.e., with results of the perturbation theory and coupled-channel calculations.

III. RESULTS

In this section we apply the finite-difference method to a collision of U^{92+} on U^{91+} at an impact energy of 10 GeV/nucleon. The electron is bound in the $1s_{1/2}$ state of the target ion at the beginning of the calculation. The projectile moves along the z axis with constant velocity v. We used a grid of 600×300 meshes with a spacing of $\Delta z = \Delta\rho = 5\times10^{-4}a_0 = 26.5$ fm. The lengths of the time steps were taken as $\Delta t = 2\times10^{-2}$ [units: $\hbar/(mc^2) = 1.288\times10^{-21}$ sec]. Then the projectile needs about 3.5 time steps to move through one cell of the grid. The radii of the nuclei are chosen as $R_T = R_P = 10^{-3}a_0 = 53$ fm, which is much larger than the physical radius of a U nucleus, but, as mentioned before, guarantees a stable solution. Three grid points are affected by this correction.

The analytic solution of the target Hamiltonian for the $1s_{1/2}$ bound state [22] is initialized on the grid and the time evolution is calculated during the time from -8.5 to $+11$. Figure 1 shows the absolute square of the wave function in the ρz plane at times $t=-8$, 0, 6, and 11. The projectile moves from the right- to the left-hand side and is located at $z=-3.1$, $0, 2.3$, and 4.2×10^3 fm, respectively. The essentially undisturbed $1s_{1/2}$ bound state is changed by the projectile potential during the time. The graphs in Fig.1 show that the wave function is contained within the grid, because the whole size of the grid is -7935 fm $\leq z \leq 7935$ fm, $\rho\leq 7935$ fm. A major part of the wave function follows the projectile, which corresponds to large ionization and pair production probabilities with high linear momentum of the ionized electron or created positron in the forward direction. This part will be analyzed by Sommerfeld-Maue functions. The outgoing spherical waves belong to ionization and pair production at low energy and will be analyzed by exact solutions of the target Hamiltonian with good angular momenta.

If we calculate the sum of the probabilities for excitation, ionization, and pair production with capture with the exact solutions summed up to $|\kappa| = 10$, the total probability is 0.884 at $t=11$. This means that states with higher values of κ are excited. In Fig. 2 the differential probabilities $dP_i^{\mathrm{ex}}(t)/dE$ and $dP_p^{\mathrm{ex}}(t)/dE$ are plotted for $t=0$ and 11 as functions of energy. The summation over the quantum number κ runs up to $|\kappa|=5$ (solid curves) and $|\kappa|=10$ (dotted curves), respectively. The total probability is 0.986 at $t=0$. This shows that we can expand the wave function into the exact solutions with $|\kappa|\leq 10$ up to $t=0$. At times larger than zero an increasing part of the probability goes to higher κ values ($|\kappa|>10$) and higher energies (up to several MeV).

As already mentioned, a more useful description of ionization and pair production with high linear momenta can be attained by projecting with Sommerfeld-Maue functions. The differential probabilities obtained with these functions and defined in Eq. (11) are also shown in Fig. 2 by crosses connected by interpolating dashed curves. Whereas the probabilities for $t=0$ are similar to those calculated with the exact wave functions, the dashed and dotted curves for $t=11$ differ already for electron energies around 1 MeV indicating that higher angular momenta are involved.

In order to calculate the total probabilities we used Eqs. (12) and (13) with $E_0 = 2$ MeV and integrated over the dashed curves in Fig. 2. We obtained $P = P_{1s_{1/2}} + P_e + P_i + P_p = 1.011$ and 1.106 for $t=0$ and 11, respectively, in comparison with 0.986 and 0.884 calculated with the exact wave functions. Values larger than 1 arise from the nonorthogonality of the Sommerfeld-Maue functions. This shows that we can describe ionization and pair production only up to $t=0$ with the exact eigenfunctions with κ values lower than 10 and that the projection amplitudes for higher κ values increase with time. We get large probabilities for ionization and pair production with high linear momenta (up to 10 MeV/c) for the ionized electron and the positron. This situation can satisfactorily be described by Sommerfeld-Maue functions, although the nonorthogonality of these functions results in a slight overestimation of the ionization and pair production probabilities.

Figure 3 shows the probabilities for excitation, ionization, and pair production with capture as a function of time t. The solid curves represent the values obtained by summing in Eq. (6) over $|\kappa| \leq 5$. Values for the probabilities obtained with Eqs. (12) and (13) were only calculated for $t = 0, 6$, and 11 because of limited computer time. They are shown by the full dots. All probabilities are compared with those of a calculation using perturbation theory (dashed curves) and of a coupled-channel calculation (dotted curves). These curves prove the strongly nonperturbative character of pair production in relativistic collisions of very heavy ions. We get a probability for pair production which is about two orders of magnitude larger than the value obtained with perturbation theory. Further we have fair agreement with results of the coupled-channel calculation, which is also nonperturbative. A similar enhancement in the pair-production probability obtained by a nonperturbative B-spline method was also found by Strayer and Bottcher [8].

The difference between our results and the results of the coupled-channel calculation in the ionization probability is due to the restricted basis set which was taken into account in the coupled-channel calculation. An extension of the basis set to higher excited bound states

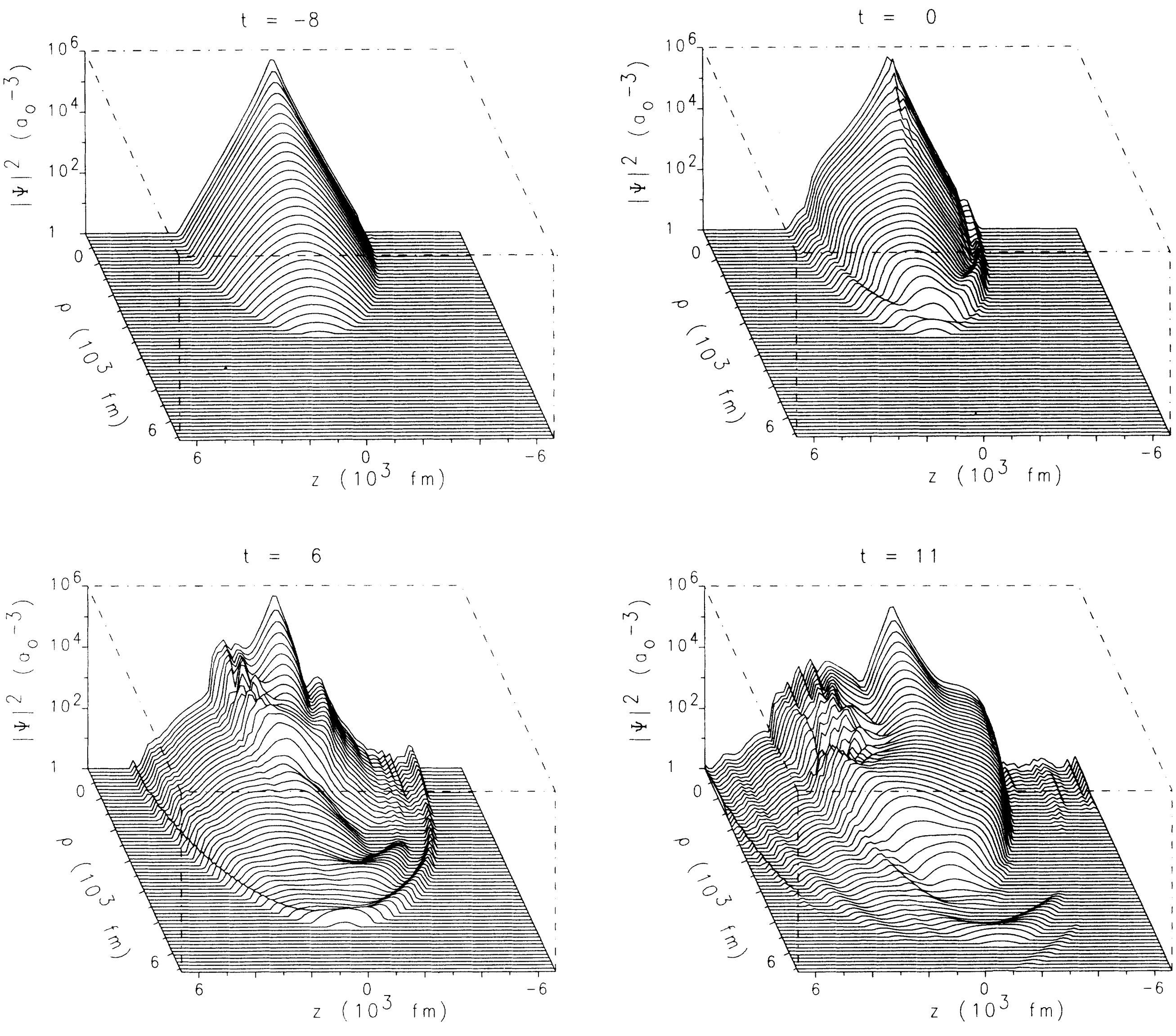

FIG. 1. Probability density of the time developed wave function of the electron at times $t = -8$, 0, 6, and 11 [units: $\hbar/(mc^2) = 1.288 \times 10^{-21}$ sec] for a nearly central collision of U^{92+} on U^{91+} with an incident energy of $E_{\rm lab} = 10$ GeV/nucleon. The projectile moves from the right- to the left-hand side and is located at $z = -3.1$, $0, 2.3$, and 4.2×10^3 fm, respectively. The density is given in units of a_0^{-3} ($a_0 = 5.3 \times 10^4$ fm).

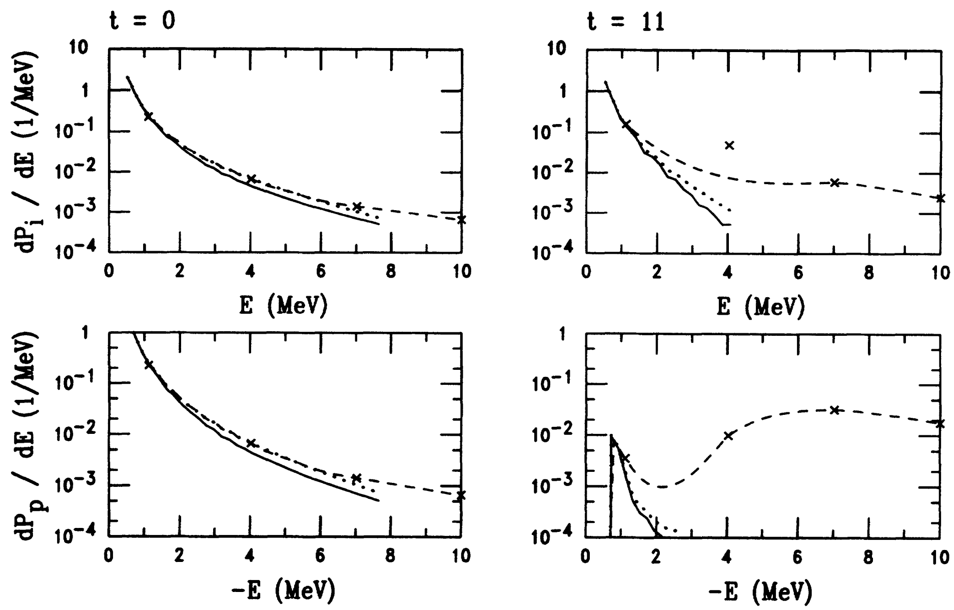

FIG. 2. Differential probability dP_i/dE for ionization and dP_p/dE for pair production with capture at times $t = 0$ and 11 [units: $\hbar/(mc^2) = 1.288 \times 10^{-21}$ sec] for a nearly central collision of U^{92+} on U^{91+} and U^{92+}, respectively. The solid and dotted curves show the results obtained with Eq. (6) by projecting on exact eigenfunctions of the target Hamiltonian. The partial probabilities are summed up to $|\kappa| = 5$ (solid curves) and $|\kappa| = 10$ (dotted curves). Results calculated by projecting with Sommerfeld-Maue functions are shown by crosses. The dashed lines are obtained by interpolating the crosses and are used for the integration over the energy.

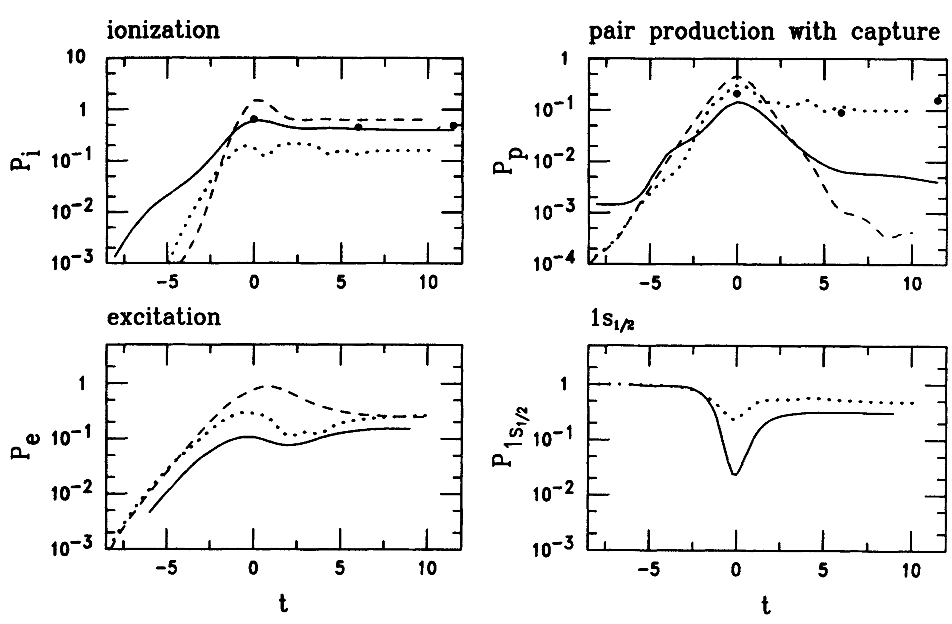

FIG. 3. The probability for ionization (P_i), pair production with capture (P_p), excitation (P_e), and occupation of the $1s_{1/2}$ bound state ($P_{1s_{1/2}}$) for nearly central collisions of U^{92+}(10 Gev/nucleon) on $U^{91+}(1s_{1/2})$ and U^{92+}, respectively, are shown as functions of time. The unit of time is 1.288×10^{-21} sec. The solid curves are calculated by projecting with exact eigenfunctions of the target Hamiltonian up to $|\kappa| = 5$. In the case of pair production and ionization also values are calculated by projecting with Sommerfeld-Maue functions which are shown by full dots. The results are compared with those obtained by first-order perturbation theory (dashed curves) and coupled-channel calculations (dotted curves).

increases the ionization probability, whereas the probability for pair production remains essentially unchanged. This increasing ionization probability is connected with a decreasing probability of the bound states, especially of the $1s_{1/2}$ bound state, which confirmes the reasonable agreement in the results of our and the coupled-channel calculation.

IV. SUMMARY

Ionization, excitation, and pair production with capture were calculated with a nonperturbative finite-difference method. As result we have found a large probability to create positrons with high linear momentum. Our results are in good agreement with coupled-channel calculations and predict a probability for pair creation with capture of 0.16 for nearly central collisions of U^{92+} on U^{92+} at an incident energy of $E_{\text{lab}} = 10$ GeV/nucleon. This value is about two orders of magnitude larger than the result of first-order perturbation theory, which shows the strongly nonperturbative character of relativistic scattering of very heavy ions with small impact parameters.

ACKNOWLEDGMENTS

This work was supported by BMFT (06 GI 709), GSI (Darmstadt), and HLRZ (Jülich).

[1] H. Gould, Lawrence Berkeley Laboratory Technical Information, Report No. LBL 18593 UC-28 (1984).
[2] G. Soff, in *Proceedings of the XVIII Winter School, Selected Topics in Nuclear Structure, Bielsko-Biala, Poland, 1980*, edited by A. Balanda and Z. Stachura (Institute of Nuclear Physics, Krakow, Poland, 1980), Report No. 1134/PL, p. 201.
[3] C. A. Bertulani and G. Baur, Nucl. Phys. A **458**, 725 (1986).
[4] C. A. Bertulani and G. Baur, Phys. Rep. **163**, 299 (1988).
[5] U. Becker, N. Grün, and W. Scheid, J. Phys. B **19**, 1347 (1986); J. Phys. **B20**, 2075 (1987).
[6] M. J. Rhoades-Brown, C. Bottcher, and M. R. Strayer, Phys. Rev. A **40**, 2831 (1989).
[7] G. Deco and N. Grün, Phys. Lett. A **143**, 387 (1990).
[8] M. R. Strayer, C. Bottcher, V. E. Oberacker, and A. S. Umar, Phys. Rev. A **41**, 1399 (1990); C. Bottcher and M. R. Strayer, in *Physics of Strong Fields*, edited by W. Greiner (Plenum, New York, 1987), p. 629; Phys. Rev. Lett. **54**, 669 (1985).
[9] K. Momberger, N. Grün, and W. Scheid, Z.Phys. D **18**, 133 (1991).
[10] K. Rumrich, W. Greiner, and G. Soff, Phys. Lett. A **149**, 17 (1990).
[11] K. Rumrich, K. Momberger, G. Soff, W. Greiner, N. Grün, and W. Scheid, Phys. Rev. Lett. **66**, 2613 (1991).
[12] N. Toshima and J. Eichler, Phys. Rev. A **38**, 2305 (1988); **40**, 125 (1989); J. Eichler, Phys. Rep. **193**, 167 (1990).
[13] G. Mehler, G. Soff, K. Rumrich, and W. Greiner, Z. Phys. D **13**, 193 (1989).
[14] K. Momberger, N. Grün, W. Scheid, and U. Becker, J. Phys. B **23**, 2293S (1990).
[15] C. Bottcher and M. R. Strayer, Phys. Rev. D **39**, 1330 (1989).
[16] G. Baur and C. A. Bertulani, Phys. Rev. C **35**, 836 (1987).
[17] E. Papageorgiu, Phys. Rev. D **40**, 92 (1989).
[18] G. Baur, *Proceedings of the CBPF International Workshop on Relativistic Aspects of Nuclear Physics*, edited by T. Kodama *et al.* (World Scientific, Singapore, 1990), p. 127; Phys. Rev. D **42**, 5736 (1990).
[19] M. J. Rhoades-Brown and J. Weneser, Phys. Rev. A **44**, 330 (1991).
[20] C. Best, W. Greiner, and G. Soff, Gesellschaft für Schwerionenforschung Report No. GSI-91-55 (1991).
[21] U. Becker, N. Grün, and W. Scheid, J. Phys. B **16**, 1967 (1983); U. Becker, N. Grün, W. Scheid, and G. Soff, Phys. Rev. Lett. **56**, 2016 (1986).
[22] E. M. Rose, *Relativistic Electron Theory* (Wiley, New York, 1961).
[23] A. Sommerfeld and A. W. Maue, Ann. Phys. (Leipzig) **22**, 629 (1935).
[24] W. H. Furry, Phys. Rev. **46**, 391 (1934).
[25] H. A. Bethe and L. C. Maximon, Phys. Rev. **93**, 768 (1954).